© Pol J Radiol 2022; 87: e641-e651
DOI: https://doi.org/10.5114/pjr.2022.121763

Received: 14.05.2022
Accepted: 07.07.2022
Published: 30.11.2022

Polish Journal of Radiology

http://www.polradiol.com

Review paper

# Comparative imaging findings among different primary betacoronaviruses

Wilson Sharp[1,E,F], Isabel Jang[2,E,F], Michael J. Diaz[3,E], Leila C. Tou[4,E], Charles A. Agyemang[5,F], Rebekah E. Carter[3,F], Sarah Sevigny[1,E], Muhammad Umair[6,E]

[1]Campbell University School of Osteopathic Medicine, USA
[2]Boston University, USA
[3]College of Medicine, University of Florida, Gainesville, FL, USA
[4]Charles E. Schmidt College of Medicine at Florida Atlantic University, USA
[5]The Johns Hopkins University, Zanvyl Krieger School of Arts and Sciences, USA
[6]The Johns Hopkins Hospital, USA

## Abstract

**Purpose**: Coronaviruses (CoV) are single-stranded RNA viruses that transmit from animal species to humans, causing a threat to global health. We aim to summarize common imaging findings of 3 betacoronaviruses (β-CoVs) and the common clinical manifestation, to provide a better understanding of the courses of the disease.

**Material and methods**: The Pubmed and Google Scholar databases were searched for the terms "SARS-CoV" OR "COVID-19" OR "MERS-CoV". Imaging-specific searches included keyword searches for "CT" AND "imaging". Clinical presentation-specific searches included keyword searches for "clinical" AND "manifestation" AND "cardiovascular" OR "neurology" OR "gastrointestinal" OR "hematology". In total, 77 articles were selected for discussion in the current literature review.

**Results**: Human β-CoVs infection presented consistent indications of ground-glass opacities (GGO), consolidation, and interlobular septal thickening. Pleural effusion was also common in all 3 β-CoVs, but it was least present in SARS-CoV-2 infection. Bilateral lung involvement was common to both MERS-CoV and SARS-CoV-2 infection. Cardiovascular, neurological, haematological, and gastrointestinal were common clinical presentations found in patients infected with β-CoVs.

**Conclusions**: The comparison of imaging findings can be applied in clinical practice to distinguish the 3 CoV through different imaging modalities. It is crucial to understand the possible imaging findings and clinical presentations to better understand the course of the disease as well as prepare for future variants.

**Key words**: coronavirus, imaging, chest, cardiovascular, gastrointestinal, haematology.

## Introduction

Coronaviruses (CoV) are single-stranded RNA viruses that repeatedly cross between species and emerge into human pathologies [1]. Betacoronaviruses (β-CoVs) – SARS-CoV-1, MERS-CoV, SARS-CoV-2 – are grouped together based on their genetic makeup and antigenic cross-reactivity, and they have the unique tendency to be transmitted from bats to humans [2]. The emergence of SARS-CoV-1 in 2002 and MERS-CoV in 2012 resulted in zoonosis from bats as a threat to global health [3]. In December 2019, a novel β-CoVs identified as severe acute respiratory syndrome coronavirus 2 (SARS-CoV-2) emerged in Wuhan, China. The constellation of symptoms caused by SARS-CoV-2 is called COVID-19. Studies have identified SARS-CoV-2 as

**Correspondence address:**
Isabel Jang, Boston University, e-mail: ijang@bu.edu

**Authors' contribution:**
**A** Study design · **B** Data collection · **C** Statistical analysis · **D** Data interpretation · **E** Manuscript preparation · **F** Literature search · **G** Funds collection

the same β-CoVs lineage as SARS-CoV-1 and MERS-CoV [1]. However, when comparing there are significant differences in the genomic sequences among the 3 β-CoVs. The major difference is found in the sequence for the receptor-binding domain between SARS-CoV-2 and SARS-CoV-1. The greater infectivity of SARS-CoV-2 may be due to the new mutations and the acquisition of the furin cleavage site that enhances the ability of the virus to internalize into the cells [4].

COVID-19 is the new infectious disease caused by SARS-CoV-2. The virus is easily transmitted human-to-human by the spread of respiratory droplets or aerosols from actions such as coughing and sneezing [5]. Most COVID-19 patients present flu-like symptoms; however, few patients develop respiratory failure, multiple organ failure, and even death. By the end of 2021, there were over 300 million confirmed cases globally, including over 5 million deaths [6].

### Diagnostic techniques

Reverse transcription polymerase chain reaction (RT-PCR) is one of the detection techniques for SARS-CoV-2 RNA. However, RT-PCR specificity for SARS-CoV-2 is subject to limitations including insufficient viral load, failure in diagnostic kits, and nonstandard sampling techniques [7]. Treanor *et al.* observed that limited use of computed tomography (CT) at the onset of the COVID-19 pandemic was due to the low specificity of chest CT scanning for COVID-19 [8], which has since improved [9]. Specifically, Shao *et al.* reported that chest CT specificity for COVID-19 increased from September 2020 (specificity = 18.1%, sensitivity = 86.2%) to March 2021 (specificity = 80.1%, sensitivity = 87.9%) ($n$ = 2346, $n$ = 16,133, respectively) [9]. The improvement in specificity and sensitivity can be attributed to the increasing knowledge surrounding COVID-19, and the implementation of formal scoring systems that clearly indicate positive findings [9]. Moreover, deep learning neural networks may improve the specificity of COVID-19 imaging, although they are not ready for clinical application at the time of writing. Many other studies have also suggested the potential of convolutional neural networks to aid in distinguishing COVID-19 pneumonia from other viral pneumonia and normal lungs based on X-ray imaging. Nikolaou *et al.* described the use of a CNN algorithm that differentiated COVID-19 from other viral pneumonia and normal lungs using chest radiography, with 93% accuracy, 94% sensitivity, and 95% specificity ($n$ = 15,153) [10]. For instance, Chaudhary *et al.* (95% accuracy and 100% sensitivity) and Luz *et al.* (90% accuracy and 93.5% sensitivity) described high accuracy and sensitivity in differentiating COVID-19 from non-COVID-19 using normal X-rays with the aid of CNN [11,12]. Chaddad *et al.* employed CNN architectures to achieve 82.3% accuracy in differentiating between COVID-19 and normal lung CT images from 60 patients infected with SARS-CoV-2 [13]. Polsinelli *et al.* also discriminated COVID-19 CT images with CNN with 83% accuracy and 85% sensitivity [14]. Considering the findings from these studies, the advent of deep learning neural networks may improve the accuracy and sensitivity of the chest X-ray and chest CT scans and increase the utility of chest X-rays in the early diagnosis of COVID-19.

Similar imaging findings exist between the 3 viral strains. For example, ground-glass opacities (GGOs), consolidation, and interlobular septal thickening are common to the 3 β-CoVs [15-19]. The presence of key distinctions, such as the predilection of bilateral lung involvement in SARS-CoV-2 and MERS-CoV infection [20], and markedly common unilateral involvement associated with SARS-CoV-1 infection, are also extensively described in the available literature [18,21]. Damage to the lungs and the occurrence of cardiovascular disease were common in all 3 β-CoVs. Common sequelae involved the gastrointestinal system, nervous system, and the haematological presentation of those infected.

The purpose of this review was to present a comprehensive understanding of the similarities and differences that are known to exist between β-CoVs that have caused pandemics, with a focus on imaging characteristics. The researchers intend for this to provide clinicians with useful insight into the clinical and imaging features of different β-CoVs and to provide a framework for future comparative studies.

## Material and methods

We searched the PubMed and Google Scholar databases for articles published between May 2003 and December 2021. All conducted keyword searches included the keyword query "SARS-CoV" OR "COVID-19" OR "MERS-CoV". Imaging-specific searches included keyword search queries for "CT" AND "imaging". Clinical presentation-specific searches included keyword search query "clinical" AND "manifestation" AND "chest" OR "lungs" OR "neurology" OR "gastrointestinal" OR "hematology". We decided to also include non-English sources because the outbreaks related to all β-CoVs affected populations globally, especially in non-English populations in past β-CoVs outbreaks. Exclusion criteria included original research articles with a sample size smaller than 10 and other systematic reviews comparing the 3 β-CoVs. Seventy-seven articles were selected for discussion in the current literature review. The authors WS and IJ searched and selected referenced studies, and MD resolved any article selection disputes.

## Results

### Chest imaging findings

Tables 1 and 2 report the hallmark and frequency, respectively, of chest CT imaging findings for SARS-CoV-1, SARS-CoV-2, and MERS-CoV infection. Human β-CoV infection consistently revealed GGOs and consolidation.

**Table 1.** Comparative chest imaging findings of patients infected with SARS-CoV-1, MERS-CoV, and SARS-CoV-2

| Author | Beta-CoV type | Imaging modality | Findings |
|---|---|---|---|
| Sotoudeh H, Gity M (2021) [7] | SARS-CoV-2 | Chest radiograph (CXR) | Multiple foci GGOs, consolidations in peripheral and lower lungs |
| Sotoudeh H, Gity M (2021) [7] | SARS-CoV-2 | Chest CT | GGOs, consolidation, crazy paving pattern, pulmonary vascular enlargement, air bronchograms, thickening of interlobular septa, pleural effusion and thickening, diffuse pulmonary involvement, lung cavitary lesions, parenchymal calcification |
| Li *et al*. (2020) [17] | SARS-CoV-2 | Chest CT | GGOs, linear opacities, consolidation, interlobular septal thickening, crazy paving pattern, bronchial wall thickening |
| Song *et al.* (2020) [28] | SARS-CoV-2 | Chest CT | GGOs, consolidation, air bronchograms, reticulation, small pleural effusion, small pericardial effusion, lymphadenopathy |
| Lan *et al.* (2015) [21] | MERS-CoV | CXR | Bilateral lung involvement, large patchy consolidation, lower lung lesions |
| Ajlan *et al.* (2014) [20] | MERS-CoV | Chest CT | Unilateral and bilateral abnormalities, GGOs consolidation, centrilobular nodules, septal thickening, peri-lobular opacities, reticulation, architectural distortion, subpleural bands, traction bronchiectasis, bronchial wall thickening, and pleural effusions |
| Das *et al.* (2015) [23] | MERS-COV | CXR | GGOs, consolidation, irregular linear airspace disease, air bronchogram, multicentric cavitation, pleural effusion |
| Hsieh *et al.* (2004) [26] | SARS-CoV-1 | CXR | Multifocal and unifocal involvement, consolidations, GGOs, pleural effusion |
| Muller *et al.* (2004) [15] | SARS-CoV-1 | Chest CT | Unilateral and bilateral GGOs, consolidation, thickening of interlobular septa |

GGOs – ground-glass opacities

**Table 2.** Frequency of radiological findings at presentation

| Radiological features | SARS-COV-1 | SARS-CoV-2 | MERS-CoV |
|---|---|---|---|
| Ground glass opacities | 82.0% [21] | 72.0-94.5% [15,26] | 66.0% [22] |
| Interlobular septal thickening | N/A | 15.1%-62.7% [9,12] | 26.0-40.0% [11,13] |
| Unilateral lung involvement | 50.0% [14] | 21.8-50.0% [3,15] | 14.0% [10] |
| Crazy paving pattern | 36.4% [11] | 12.0-36.1% [9,11,12,15] | 27.0% [11] |
| Pleural effusion | 15.0-22.7% [11,22,23] | 3.0-4.0% [15,20] | 30.0%-60.0% [11,22,23] |

N/A – not applicable, i.e. lack of data in a form or table.

Wang *et al*. reported GGO in 82% (92/112) and mixed air-space opacities with irregular consolidation in 21% (24/112) of SARS-CoV-1-infected patients [22]. Das *et al.* identified GGO in 66% (36/55), with consolidation in 18% (10/55) of MERS-CoV-infected patients [23]. By comparison, Xu *et al*. reported GGO in 72% (65/90), with consolidation in 13% (12/90) of SARS-CoV-2-infected patients [19]. A sister review of SARS-CoV-2 infection reported 94.5% incidence of GGO with or without consolidation ($n$ = 55) [24].

Pleural effusion was identified among cases for all described β-CoVs, but it was least common in SARS-CoV-2 infection [25]. Das *et al*. and Hsieh *et al.* reported that 15% of SARS-CoV-1 and 30% of MERS patients developed pleural effusion, respectively ($n$ = 26, $n$ = 55) [23,26]. Interestingly, Xu *et al.* reported pleural effusion in only 4% of SARS-CoV-2-infected patients ($n$ = 90) [19]. Wong *et al*. also corroborated its rarity, observing pleural effusion in a mere 3% (2/64) of SARS-CoV-2 patients ($n$ = 64) [27].

Crazy-paving pattern [17,19] was uniquely identified in SARS-CoV-2 infection cases. One study found crazy-paving patterns in 36% of SARS-CoV-2-infected patients (30/$n$ = 83) compared to another study that reported 12% of patients (11/$n$ = 90) [17,19]. Although the literature is sparse, a comparable difference is described for the finding of air bronchogram between patients infected with SARS-CoV-2 and MERS-CoV. Song *et al*. reported that 80% of SARS-CoV-2-infected patients had air bronchogram ($n$ = 51) [28]. Das *et al*. reported air bronchogram in only 11% of MERS-CoV-infected patients ($n$ = 55) [23].

Bilateral lung involvement is common to both MERS-CoV and SARS-CoV-2 infection. According to Ajlan *et al*., 86% (6/7) of MERS-CoV-infected patients experience bilateral lung involvement [20]. Huang *et al.* reported 97.5% of the initial chest radiographs from patients infected with SARS-CoV-2 presented with bilateral involvement ($n$ = 41), as shown in Figures 1 and 2 [18]. One of the common findings that distinguished SARS-CoV-1 from both MERS-CoV and SARS-CoV-2 is the predominance of

**Figure 1.** Non-contrast axial chest computed tomography (CT) of a 60-year-old female patient diagnosed with COVID-19. Presentation of multilobar and bilateral ground-glass opacities with lobular and rounded morphology mostly in the periphery of both lungs. Case courtesy of Dr Bahman Rasuli, Radiopaedia.org, rID: 74560

**Figure 2.** Chest computed tomography (CT) of a 40-year-old female patient diagnosed with COVID-19. Presentation of multifocal bilateral patchy and confluent ground-glass opacities with crazy paving on both lungs. Case courtesy of Dr Bahman Rasuli, Radiopaedia.org, rID: 93230

unilateral lung involvement [15,29]. According to Wong *et al.*, based on chest radiographs, unifocal involvement (54.5%) was more prevalent compared to bilateral involvement (38.0%) in patients infected with SARS-CoV-1 ($n$ = 108) [29]. In another study conducted by Müller *et al.*, during the initial presentation of the disease, CT findings showed more prevalent unilateral GGOs than bilateral (50% vs. 16.7%) among a sample size of 12 [15]. However, as the disease progressed, follow-up CT scans obtained after 2-27 days (median, 9 days) of hospitalization showed a greater percentage of bilateral involvement compared to unilateral for GGOs (52% vs. 8%) and consolidation (20% vs. 8%) ($n$ = 25) [15].

## Cardiovascular imaging findings

Clinical features include hypertension [30-32], acute myocarditis [33-35], and coronary heart disease [34]. Abnormal echocardiography was found in 55% (667/$n$ = 1216) of SARS-CoV-2-infected patients [36]. Left (39%) and right (33%) ventricular abnormalities, myocardial infarction (3%), and myocarditis (3%) were reported ($n$ = 1216) [36]. When comparing the echocardiographic findings of SARS-CoV-1 patients in the acute stage of infection compared to 30 days later, patients exhibited diastolic impairment with left ventricular systolic involvement upon infection [37]. Patients reported with lower mean left ventricular ejection fraction (65.3 ± 12.8% vs. 71.4 ± 5.7%, $p$ = 0.03) and higher mean index of myocardial performance (0.51 ± 0.11 vs. 0.40 ± 0.12, $p$ = 0.017) [37].

Common cardiac magnetic resonance (CMR) findings in patients infected with SARS-CoV-2 include myocardial oedema, pericardial effusion, late gadolinium enhancement (LGE) in the myocardium, global higher T1 and T2 relaxation time, and elevated extracellular volume (ECV) percentage [33-35]. Participants of the study conducted by Luetkens *et al.* were infected with SARS-CoV-2 and were suspected myocarditis cases experiencing dyspnoea and fever, exhibiting positive radiographic findings of COVID pneumonia on chest CT or radiograph [33]. 38% of participants had small pericardial effusions, and 88% of patients had LGE present in the sub-epicardium of the lateral wall or in the basal septal midmyocardium [33]. Higher T1 and T2 relaxation times were seen in patients compared to healthy controls (T1, 1046 vs. 953 ms; T2, 61.7 vs. 52.9 ms) [33]. The ECV for COVID-19 patients was elevated compared to healthy controls (29.2% vs. 28.1%); however, the data were not significantly different ($p$-value 0.25) [33]. Simi-

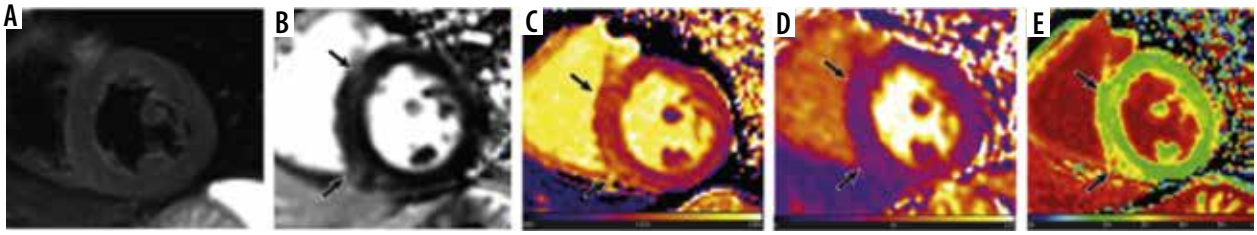


**Figure 3.** Cardiac magnetic resonance of a 60-year-old male COVID-19 patient 2 months after the onset of palpitations. **A**) Short-axis short tau inversion recovery (STIR) sequence shows no signs of myocardial oedema. However, (**B**) phase-sensitive inversion recovery (PSIR) image shows evidence of focal late gadolinium enhancement (LGE) in left ventricular septal and inferior segments (black arrows). Increased native T1 (1434 ± 43 ms), extracellular volume (ECV) (30 ± 2%), and normal T2 values (38 ± 2 ms) were shown in the corresponding location of focal LGE on the T1 (**C**), T2 (**D**), and ECV maps (**E**) (black arrows)

larly, in another study conducted by Huang *et al.* (2020), CMR findings consisted of myocardial oedema (54%), positive LGE (58%), and elevated T1, T2, and ECV ($n$ = 26), as shown in Figure 3 [35]. 60% of the patients observed with positive late gadolinium enhancement exhibited lesions located sub-epicardium of the inferior and inferior-lateral segments at the base and mid-chamber [35]. Comparing patients with positive CMR findings to patients without positive findings and healthy controls, T1, T2, and ECV values were elevated (T1, 1,271 vs. 1,237 vs. 1,224 ms; T2, 42.7 vs. 38.1 vs. 39.1 ms; ECV, 28.2% vs. 24.8% vs. 23.7%) [35]. In an observational cohort study, researchers reported that CMR revealed cardiac involvement in 78% of patients and ongoing myocardial inflammation in 60% of COVID patients who recovered from lower left ventricular ejection fraction (LVEF), higher left ventricle volumes, and raised native T1 and T2 ($n$ = 100) [38]. It is important to note that this data are obviously a representation of the COVID patients who presented with heart failure with low LVEF and left ventricular chamber dilation, and they are not applicable to all COVID patients. Compared to healthy controls, patients exhibited raised myocardial native T1 (73/100) and T2 (60/100), myocardial LGE (32/100), and pericardial enhancement (22/100) [38]. In comparison, not enough literature exists on the cardiac magnetic resonance imaging (MRI) findings of the remaining 2 β-coronaviruses.

Contrast-enhanced CT pulmonary angiograms (CTPA) in patients infected with SARS-CoV-2 exhibited dilated pulmonary vasculature in 85% of cases (41/45) [39]. Venous thromboembolism, including pulmonary pmbolism (PE) and deep vein thrombosi (DVT), are frequent findings in SARS-CoV-2-infected patients. Patients infected with SARS-CoV-2 are likely to have venous and arterial thromboembolism due to excessive inflammation, hypoxia, immobilization, and diffuse intravascular coagulation [40]. In a study conducted by Cui *et al.*, 25% (20/81) of SARS-CoV-1-infected patients were diagnosed with venous thromboembolism (VTE) [41]. Similarly, a study conducted by Klok *et al.* reported a composite outcome of 31% of which CTPA confirmed VTE (27%) [42]. Noncompressible veins, echogenic clots, and minimal or absent flow within a swollen vein were common imaging findings for DVT among these patients, and not different from patients with DVT from any aetiology [43].

Contrarily to SARS-CoV-2 cases, reports of PE are less frequent for SARS-CoV-1 cases, which may suggest a lower incidence of thromboembolic phenomena among those viruses; however, insufficient literature currently exists to reach this conclusion. Although coagulation abnormalities are common in SARS-CoV-1 patients, thromboembolic events are rarely detected. Ng *et al.* reported the first case of pulmonary artery thrombosis for a SARS-CoV-1-infected patient. CT angiogram of the thorax showed GGOs in the left upper and right lower lobes, and a blood clot in the right main pulmonary artery that extended to the segmental artery of the right lower lobe [44].

## Neurological presentation

Neurological manifestation in the described β-CoVs included, but was not limited to, fatigue, headache, and reduced consciousness [45-47]. Acute cerebrovascular complications, specifically acute ischaemic stroke, are the most common COVID-19 manifestations of neurological pathologies [48]. In contrast, a study conducted by Umapathi *et al.* reported that 5 patients (2%) infected with SARS-CoV-1 experienced stroke ($n$ = 206) [49]. However, researchers suggest that a correlation between SARS-CoV-1 and stroke may be coincidental because the patients who experienced a stroke were diagnosed with multiple co-morbidities such as cardiac dysfunction, DIC, and hypertension [49]. Figure 4 shows images of non-contrast head CT from COVID-19 patients with common neuroimaging findings including multifocal ischaemic infarcts (25%), acute white matter encephalopathic changes (37.5%), and cortical or intracranial haemorrhage (6%) ($n$ = 16) [50]. Again, the contribution of the confounding factors here remains unclear.

In the comparison, brain MRIs for 3 MERS-CoV infected patients presented bilateral hyperintense lesions in the subcortical white matter of the frontal, temporal, and parietal lobes, basal ganglia, and corpus callosum, as shown in Figure 5 [51]. Another case study involving CT scans of a MERS-CoV-infected patient showed right frontal lobe intracerebral haemorrhage with massive brain oedema and midline shift [52]. For patients infected with SARS-CoV-1, there were limited abnormalities found through neuroimaging. A case study reported that an MRI examination of a SARS-CoV-1-infected patient's brain during the acute stage of SARS-CoV-1 showed no definite lesion [53]. Again, the literature is limited regarding these findings among the setting of comparison of β-CoVs.

## Haematological presentation

SARS-CoV-1, MERS-CoV, and SARS-CoV-2 have all been associated with haematological abnormalities [54-57]. For example, thrombocytopaenia incidence was reported at rates greater than 35%; a retrospective analysis reported an incidence of 55% (87/157) in SARS-CoV-1-infected patients ($n$ = 157) and an incidence of 58% (7/12) among critically ill patients infected with MERS-CoV ($n$ = 12) [55,58]. Disseminated intravascular coagulation (DIC) represented another shared consequence of β-CoV infection [52,54,59].

As the pandemic has progressed more information has been obtained on the incidence and imaging characteristics of SARS-CoV-2-associated DVT and DIC. Suh *et al.* performed a meta-analysis of 3342 SARS-CoV-2 patients and found the incidence of PE and DVT to be 16.5% and 14.8 %, respectively [60]. In the study it was noted that incidence rates were elevated among ICU-admitted patients (PE = 24.7%; DVT: 21.2%), and the studies that used

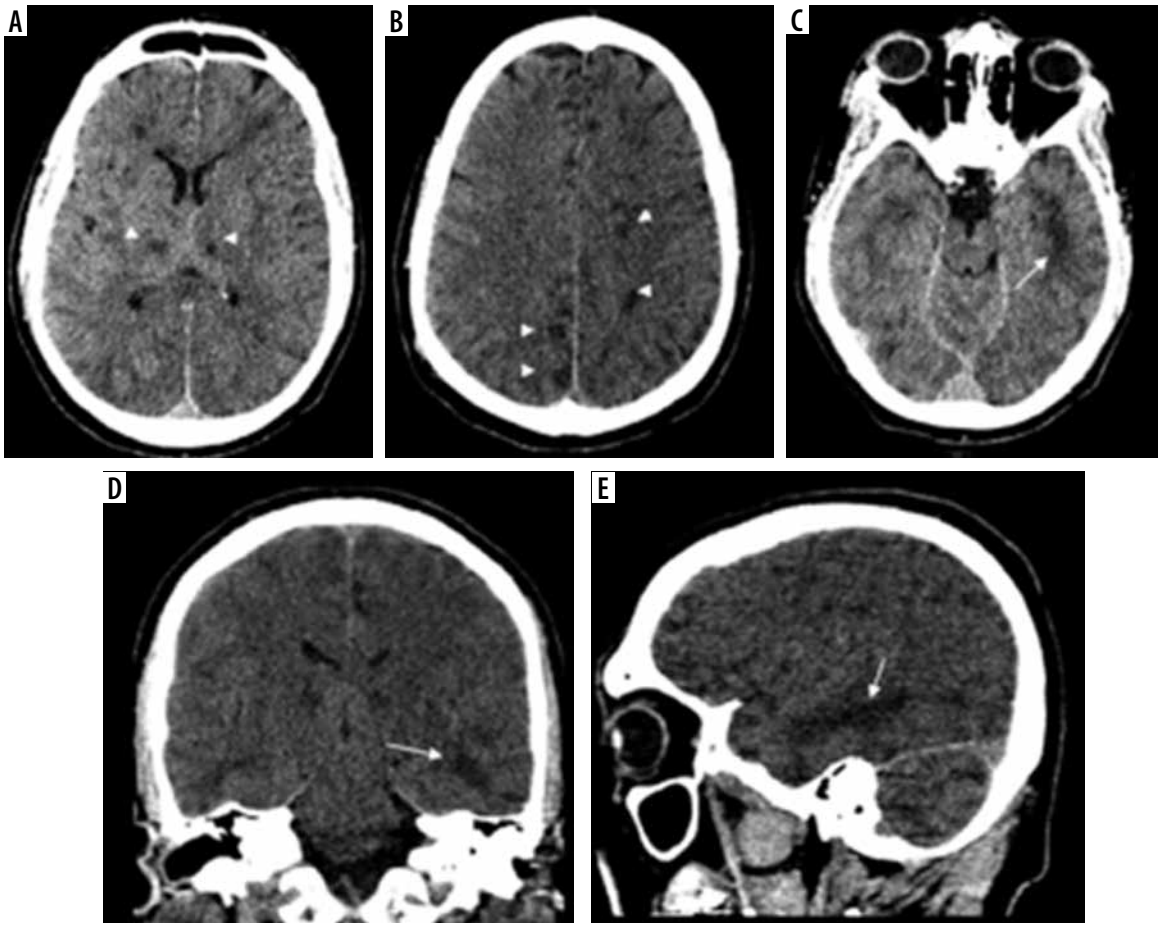


**Figure 4.** Non-contrast head computed tomography (CT) shows bilateral thalamic and scattered subcortical white matter hypodensities (arrowhead). Evidence of nonconfluent scattered subcortical and patchy white matter hypodensities with asymmetric involvement of the left temporal lobe (arrows)

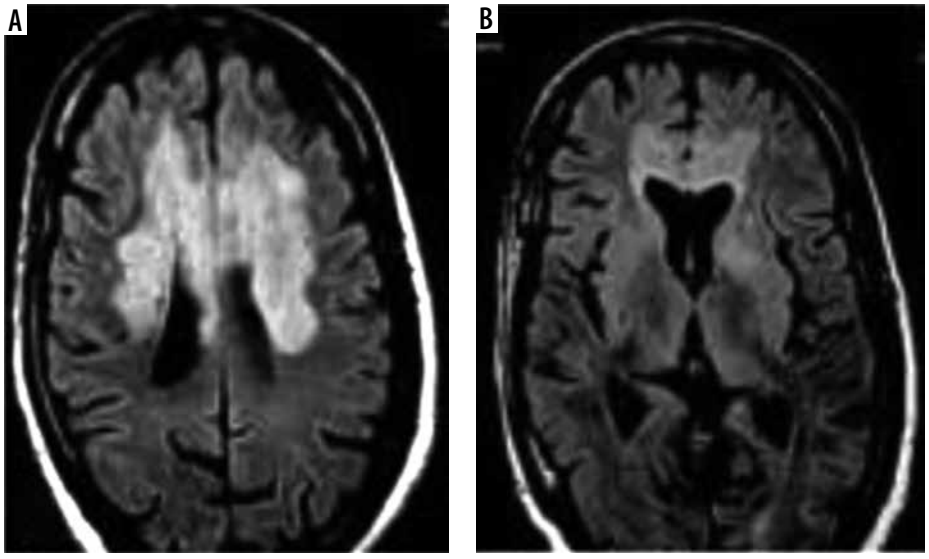


**Figure 5.** Axial FLAIR images of a 57-year-old male patient with MERS-CoV. Results showed bilateral confluent subcortical areas and deep white matter hyperintense lesions in the frontal lobes, basal ganglia, and corpus callosum

CTPA to screen all ICU admitted patients reported higher incidence rates than studies that sparingly used CTPA [60]. A sufficiently large study uniformly using CTPA to screen PE and DVT has yet to be completed, leaving the true incidence unknown. Espallargas *et al*. completed a study to describe the laboratory and imaging findings in confirmed PE-diagnosed SARS-Cov-2 patients [61]. On CTPA, the incidence of lobar PE was 25% of total cases, purely segmental in 31.25%, and subsegmental in 25%, with the right lung being affected in 93.75% of cases [61].

The available literature on both SARS-CoV-2 and SARS-CoV-1 infection corroborates findings of increased

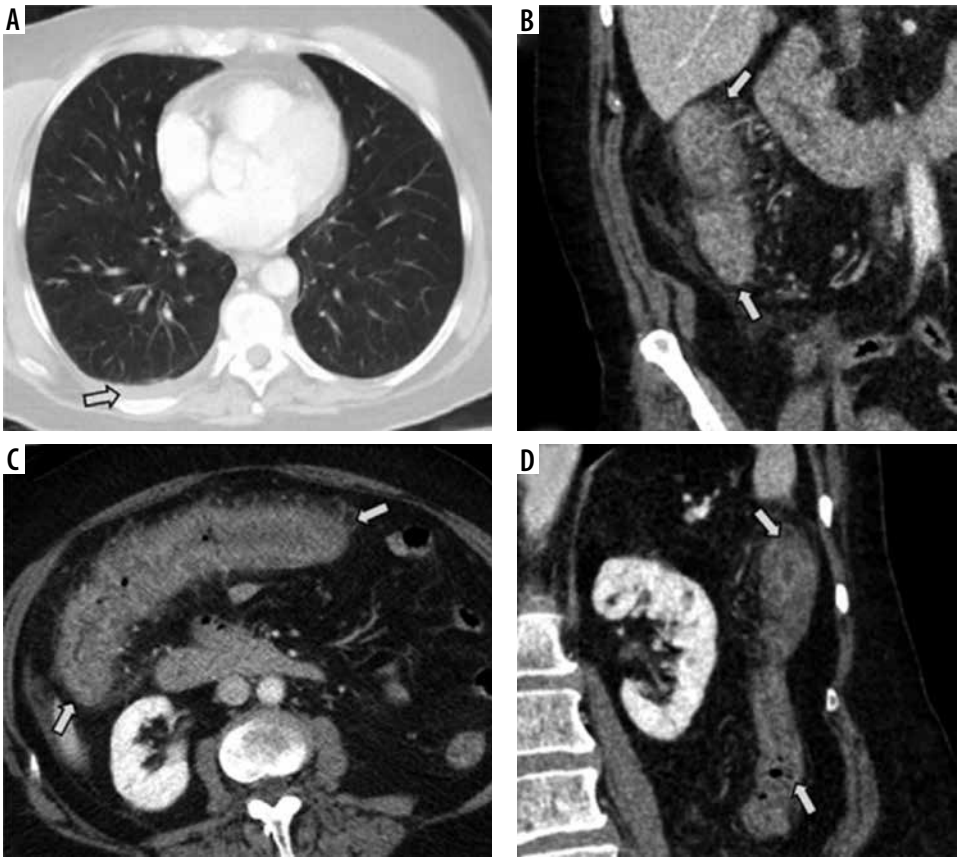


**Figure 6.** Initial computed tomography (CT) scan of the abdomen and pelvis of patients infected with SARS-CoV-2. **A**) Axial CT image of the lower thorax shows no airspace disease in the lungs. A small, right pleural effusion is present (arrow). **B-D**) Intravenous contrast-enhanced CT scan of the abdomen and pelvis in the coronal (**B** and **D**) and axial (**C**) planes shows severe inflammation of the ascending colon (**B**), transverse colon (**C**), and descending colon (**D**) characterized by circumferential wall thickening, mural hyperenhancement, mesenteric hypervascularity, and pericolic fat stranding (arrows)

D-dimer plasma levels and fibrinogen [62]. Elevated D-dimer can be related to deep vein thrombosis (DVT) and acute pulmonary embolism (PE) [63]. However, D-dimer levels alone cannot be an indicator of PE because cancer, peripheral vascular disease, pregnancy, inflammatory diseases, and other medical conditions can elevate levels [63]. Therefore, CTPA is an effective imaging technique to detect PE and its severity [64].

### Gastrointestinal presentation

All 3 β-CoV infections reported viral replication in intestinal epithelial cells and detection of viral RNA in the stool of patients with MERS-CoV and SARS-CoV-1 infection [64-67]. Infection with any of the primary β-CoVs manifested symptoms of gastrointestinal abnormality including diarrhoea, nausea, and abdominal pain during illness. Contrast-enhanced CT scans showed diffuse, circumferential, homogeneously enhancing bowel wall thickening [68]. A case study conducted with a SARS-CoV-2-infected patient showed severe colonic inflammation characterized by circumferential wall thickening in CT scan with IV contrast, as shown in Figure 6 [69]. Another retrospective cross-sectional study also reported bowel wall thickening (29%), colon or rectal thickening (17%), and small-bowel thickening (12%) ($n$ = 42) on CT scans with IV contrast [70].

## Discussion

The zoonotic action of beta-CoVs implicated concern for global health. With the recent COVID-19 pandemic, studies show how SARS-CoV-2 generates similar chest imaging abnormalities (Table 1) to its familial predecessors. However, despite its shared lineage with SARS-CoV-1 and MERS-CoV, key presentation and imaging differences do indeed exist. These differences represent opportunities for unique treatment plans, diagnostic criteria, and preparation for sequelae to avoid delayed or inappropriate care. Herein, we contrasted the available clinical and imaging features of the most notable β-CoVs to date.

The current review primarily focused on the similarities and differences in radiological findings for various known clinical presentations. Chest CT scans noted in the SARS-Cov-2 infection may appear similar to other infections including influenza virotypes, connective tissue diseases, acute lung injuries from drug reactions, and especially pathologies caused by other coronaviruses [71]. Regardless, several studies have demonstrated notable imaging findings apparent on chest CT and radiographs.

In the early stages of the disease course, findings of chest radiography and CT may range from a normal appearance to unilateral or bilateral lung opacities, which can have a basilar or peripheral distribution [72]. Several characteristics including higher incidences of bilateral lung involvement, multifocal consolidation, and crazy-paving pattern were uniquely noted in the presentation of SARS-CoV-2 infection [15,18,19,24,25,27]. While there was relatively little documentation of bilateral lung involvement in CT findings of SARS-CoV-1 infection [18], it was described markedly earlier and less frequently compared to the SARS-CoV-2 disease course [15,17-19,24,25,27]. Early lung involvement, bilateral and symmetric GGOs and consolidations and crazy-paving pattern, which is associated with ARDS on chest CT, may be consistent with a more severe presentation of SARS-CoV-2 infection compared to other beta-CoVs. As the number of patients post-hospitalization with SARS-CoV-2 continues to rise more is being uncovered, such as the presence of organizing pneumonia patterns following more prolonged or complicated disease courses [73-75]. Studies are showing the presence of common radiographic findings of organizing pneumonia (peripheral subpleural consolidations or GGOs, peri-bronchovascular opacities or thickening, nodules, masses, and interstitial opacities/septal wall thickening in similar distribution) alongside the needed histological sample that confirms its presence in SARS-CoV-2 cases [73-76].

There are similar extra-pulmonary clinical presentations across the 3 β-CoVs. Notably, patients infected with the β-CoVs exhibited cardiovascular, gastrointestinal, neurological, and haematological presentation among other systems involved.

Reports of abnormal echography are reported for patients infected with SARS-CoV-1 and SARS-CoV-2 for cardiovascular presentation [36,37]. In SARS-CoV-1 infection, results show that there are significant diastolic impairments compared to systolic [37]. Pericardial effusion, myocardial scar represented by delayed gadolinium enhancement, and abnormal T1 and T2 relaxation time, were common findings of cardiac MRI in patients infected with SARS-CoV-2. Venous thromboembolism was frequently reported in patients infected with SARS-CoV-2 with incompressible veins, echogenic clots, and minimal or absent flow within a swollen vein as common imaging findings [40-43]. CT pulmonary angiogram in patients infected with SARS-CoV-2 reported high rates of dilated pulmonary vasculature. Reports of thromboembolism were less frequent in SARS-CoV-1 [44]. Common cardiac MRI findings in patients infected with SARS-CoV-2 include myocardial oedema, pericardial effusion, LGE, and elevated T1, T2, and ECV. Even after recovery, patients who experienced cardiac symptoms continuously exhibited myocardial scar represented by LGE, and raised T1, T2, and ECV levels. At the time of writing, findings on cardiac MRI for SARS-CoV-1 and MERS-CoV are limited.

With gastrointestinal manifestation, imaging results exhibit bowel wall thickening in SARS-CoV-2 infection [64,68,69]. Although patients infected with SARS-CoV-1 and MERS-CoV reported gastrointestinal clinical manifestations, there are limited reports on the imaging findings [64-67]. Neuroimaging findings identified white matter changes and lesions common to SARS-CoV-2 and MERS-CoV [50-52]. Lastly, haematological abnormalities were present in all β-CoVs, such as thrombocytopaenia, disseminated intravascular coagulation, and venous thromboembolism [52,54,59]. Notably, SARS-CoV-1 and SARS-CoV-2 were associated with increases in acute phase reactants such as D-dimer and fibrinogen [68]. However, only SARS-CoV-2 infections reported thrombotic complications such as PE and venous thromboembolism [44].

Current challenges in diagnosing SARS-CoV-2 infection and its evolving nature could potentially lead to increased disease complications and poorer prognosis amongst cases with delayed diagnosis. Because it is difficult to differentiate SARS-CoV-2 pneumonia from many other viral respiratory infections using thoracic imaging alone, a combination of clinical manifestations, laboratory testing, and contact history should be considered in the final diagnosis.

## Limitations

The chief limitation of the current study is the consistency of available literature. Herein we examined numerous retrospective studies (e.g. systematic reviews and epidemiological data), which naturally lent themselves to methodological bias, selection bias, and confounding variables previously described by Waller *et al.* [77]. For example, many studies reported radiological evidence of SARS-CoV-2 infection only from strictly clinically symptomatic patients. Furthermore, analysis of imaging findings representing beta-CoV infection captures only a snapshot of the disease course.

## Future directions

The recent emergence of novel SARS-CoV-2 variants further underscores the need for improvements in the diagnostic methods for detecting SARS-CoV-2 infection, given its continuous evolution in the setting of a prolonged pandemic. Future investigations should examine the role of imaging in the screening of SARS-CoV-2 infection of both clinically asymptomatic and symptomatic patients, coupled with assessment of the disease course. In line with the above discussion, detection of SARS-CoV-2 infection by RT-PCR alone may still be limited. While RT-PCR kits improve, clinicians may need to interpret SARS-CoV-2 test results in the overall context of the patient's clinical presentation, aided by laboratory results and imaging findings.

## Conclusions

As of January 2022, more than 300 million cases of SARS-CoV-2 infection have been verified, and 5.5 million SARS-CoV-2-infected persons have died [6]. The key to understanding and increasing diagnostic accuracy for current and future β-CoV strains is having the best possible understanding of their clinical courses and pertinent, although subtle, imaging differences. Herein we reviewed the properties unique to and shared among the primary β-CoV – SARS-CoV-1 (2002), MERS-CoV (2012), and SARS-CoV-2 (2019) in the context of commonly involved organ systems and pertinent imaging findings.

## Conflict of interests

The authors declare no conflict of interest.

### References


1. Chan JF, Kok KH, Zhu Z, et al. Genomic characterization of the 2019 novel human-pathogenic coronavirus isolated from a patient with atypical pneumonia after visiting Wuhan. Emerg Microb Infect 2020; 9: 221-236.
2. Kaur N, Singh R, Dar Z, et al. Genetic comparison among various coronavirus strains for the identification of potential vaccine targets of SARS-CoV2. Infect Genet Evol 2021; 89: 104490.
3. Long MJC, Aye Y. Science's response to COVID-19. ChemMedChem 2021; 16: 2288-2314.
4. Hafiane A. SARS-CoV-2 and the cardiovascular system. Clin Chim Acta 2020; 510: 311-316.
5. Lotfi M, Hamblin MR, Rezaei N. COVID-19: transmission, prevention, and potential therapeutic opportunities. Clin Chim Acta 2020; 508: 254-266.
6. WHO Coronavirus (COVID-19) Dashboard. Available at: https://covid19.who.int/ (Accessed: 02.03.2022).
7. Sotodeh H, Gity M. The role of medical imaging in COVID-19. Adv Exp Med Biol 2021; 1318: 413-434.
8. Treanor L, Islam N, Ebrahimzadeh S, et al. The Cochrane systematic review on thoracic imaging tests for the diagnosis of COVID-19. Radiology 2021; 299: E289.
9. Kazi S, Absi M, Islam N, et al. Diagnostic accuracy of CT for COVID-19 Re: diagnostic accuracy of screening tests for patients suspected of COVID-19, a retrospective cohort study. Infect Dis (Lond) 2022; 54: 157-158.
10. Nikolaou V, Massaro S, Fakhimi M, et al. COVID-19 diagnosis from chest x-rays: developing a simple, fast, and accurate neural network. Health Inf Sci Syst 2021; 9: 36.
11. Chaudhary Y, Mehta M, Sharma R, et al. Efficient-CovidNet: deep learning based COVID-19 detection from chest x-ray images. In: 2020 IEEE International Conference on e-Health Networking, Application & Services (HEALTHCOM). Available at: https://ieeexplore.ieee.org/abstract/document/9398980. doi: 10.1109/HEALTHCOM49281.2021.9398980.
12. Luz E, Lopes Silva P, Silva R, et al. Towards an effective and efficient deep learning model for COVID-19 patterns detection in X-ray images. arXiv:2004.05717. doi: https://doi.org/10.48550/arXiv.2004.05717.
13. Chaddad A, Hassan L, Desrosiers C. Deep CNN models for predicting COVID-19 in CT and x-ray images. J Med Imaging (Bellingham) 2021; 8 (Suppl 1): 014502. doi: 10.1117/1.JMI.8.S1.014502.
14. Polsinelli M, Cinque L, Placidi G. A light CNN for detecting COVID-19 from CT scans of the chest. Pattern Recogn Lett 2020; 140: 95-100.
15. Müller NL, Ooi GC, Khong PL, et al. High-resolution CT findings of severe acute respiratory syndrome at presentation and after admission. Am J Roentgenol 2004; 182: 39-44.
16. Borges Do Nascimento IJ, von Groote TC, O'Mathúna DP, et al. Clinical, laboratory and radiological characteristics and outcomes of novel coronavirus (SARS-CoV-2) infection in humans: a systematic review and series of meta-analyses. PLoS One 2020; 15: e0239235.
17. Li K, Wu J, Wu F, et al. The clinical and chest CT features associated with severe and critical COVID-19 pneumonia. Invest Radiol 2020; 55: 327-331.
18. Huang C, Wang Y, Li X, et al. Clinical features of patients infected with 2019 novel coronavirus in Wuhan, China. Lancet (London, England) 2020; 395: 497-506.
19. Xu X, Yu C, Qu J, et al. Imaging and clinical features of patients with 2019 novel coronavirus SARS-CoV-2. Eur J Nucl Med Mol Imaging 2020; 47: 1275-1280.
20. Ajlan AM, Ahyad RA, Jamjoom LG, et al. Middle east respiratory syndrome coronavirus (MERS-CoV) infection: chest CT findings. Am J Roentgenol 2014; 203: 782-787.
21. Lan B, Lu P, Zeng Y, et al. Clinical imaging research of the first Middle East respiratory syndrome in China. Radiol Infect Dis 2015; 2: 173-176.
22. Wang R, Sun H, Song L, et al. Plain radiograph and CT features of 112 patients with SARS in acute stage. Beijing Da Xue Xue Bao Yi Xue Ban 2003; 35: 29-33.
23. Das KM, Lee EY, Jawder SEA, et al. Acute middle east respiratory syndrome coronavirus: temporal lung changes observed on the chest radiographs of 55 patients. Am J Roentgenol 2015; 205: W267-S274.
24. Lu L, Zhong W, Bian Z, et al. A comparison of mortality-related risk factors of COVID-19, SARS, and MERS: a systematic review and meta-analysis. J Infect 2020; 81: e18-e25.
25. Franquet T, Jeong YJ, Lam HYS, et al. Imaging findings in coronavirus infections: SARS-CoV, MERS-CoV, and SARS-CoV-2. Br J Radiol 2020; 93: 20200515.
26. Hsieh SC, Chan WP, Chien JCW, et al. Radiographic appearance and clinical outcome correlates in 26 patients with severe acute respiratory syndrome. Am J Roentgenol 2004;182: 1119-1122.
27. Wong HYF, Lam HYS, Fong AHT, et al. Frequency and distribution of chest radiographic findings in patients positive for COVID-19. Radiology 2020; 296: E72-E78.
28. Song F, Shi N, Shan F, et al. Emerging 2019 novel coronavirus (2019-nCoV) pneumonia. Radiology 2020; 295: 210-217.

29. Wong KT, Antonio GE, Hui DSC, et al. Severe acute respiratory syndrome: radiographic appearances and pattern of progression in 138 patients. Radiology 2003; 228: 401-406.
30. Quinaglia T, Shabani M, Rezaei N. COVID-19 in patients with hypertension. Adv Exp Med Biol 2021; 1318: 243-261.
31. Akpek M. Does COVID-19 cause hypertension? Angiology 2022; 73: 682-687.
32. Chen G, Li X, Gong Z, et al. Hypertension as a sequela in patients of SARS-CoV-2 infection. PLoS One 2021; 16: e0250815.
33. Luetkens JA, Isaak A, Öztürk C, et al. Cardiac MRI in suspected acute COVID-19 myocarditis. Radiol Cardiothorac Imaging 2021; 3: e200628.
34. Panchal A, Kyvernitakis A, Mikolich JR, et al. Contemporary use of cardiac imaging for COVID-19 patients: a three center experience defining a potential role for cardiac MRI. Int J Cardiovasc Imaging 2021; 37: 1721-1733.
35. Huang L, Zhao P, Tang D, et al. Cardiac involvement in patients recovered from COVID-2019 identified using magnetic resonance imaging. JACC Cardiovasc Imaging 2020; 13: 2330-2339.
36. Dweck MR, Bularga A, Hahn RT, et al. Global evaluation of echocardiography in patients with COVID-19. Eur Heart J Cardiovasc Imaging 2020; 21: 949-958.
37. Li SSL, Cheng CW, Fu CL, et al. Left ventricular performance in patients with severe acute respiratory syndrome. Circulation 2003; 108: 1798-1803.
38. Puntmann VO, Carerj ML, Wieters I, et al. Outcomes of cardiovascular magnetic resonance imaging in patients recently recovered from coronavirus disease 2019 (COVID-19). JAMA Cardiol 2020; 5: 1265-1273.
39. Lang M, Som A, Carey D, et al. Pulmonary vascular manifestations of COVID-19 pneumonia. Radiol Cardiothorac Imaging 2020; 2: e200277.
40. Azouz E, Yang S, Monnier-Cholley L, et al. Systemic arterial thrombosis and acute mesenteric ischemia in a patient with COVID-19. Intensive Care Med 2020; 46: 1464-1465.
41. Cui S, Chen S, Li X, et al. Prevalence of venous thromboembolism in patients with severe novel coronavirus pneumonia. J Thromb Haemost 2020; 18: 1421-1424.
42. Klok F, Kruip M, van der Meer N, et al. Incidence of thrombotic complications in critically ill ICU patients with COVID-19. Thromb Res 2020; 191: 145-147.
43. Revzin MV, Raza S, Warshawsky R, et al. Multisystem imaging manifestations of COVID-19, Part 1: viral pathogenesis and pulmonary and vascular system complications. Radiographics 2020; 40: 1574-1599.
44. Ng KHL, Wu AKL, Cheng VCC, et al. Pulmonary artery thrombosis in a patient with severe acute respiratory syndrome. Postgrad Med J 2005; 81: e3. doi: 10.1136/pgmj.2004.030049.
45. Noorwali AA, Turkistani AM, Asiri SI, et al. Descriptive epidemiology and characteristics of confirmed cases of Middle East respiratory syndrome coronavirus infection in the Makkah Region of Saudi Arabia, March to June 2014. Ann Saudi Med 2015; 35: 203-209.
46. Mao L, Jin H, Wang M, et al. Neurologic manifestations of hospitalized patients with coronavirus disease 2019 in Wuhan, China. JAMA Neurol 2020; 77: 683-690.
47. Beltrán-Corbellini Á, Chico-García JL, Martínez-Poles J, et al. Acute-onset smell and taste disorders in the context of COVID-19: a pilot multicentre polymerase chain reaction based case-control study. Eur J Neurol 2020; 27: 1738-1741.
48. Sklinda K, Dorobek M, Wasilewski PG, et al. Radiological manifestation of neurological complications in the course of SARS-CoV-2 infection. Front Neurol 2021; 12: 711026.
49. Umapathi T, Kor AC, Venketasubramanian N, et al. Large artery ischaemic stroke in severe acute respiratory syndrome (SARS). J Neurol 2004; 251: 1227-1231.
50. Rehmani R, Segan S, Maddika SR, et al. Spectrum of neurologic & neuroimaging manifestation in COVID-19. Brain Behav Immun Health 2021; 13: 100238.
51. Arabi YM, Harthi A, Hussein J, et al. Severe neurologic syndrome associated with Middle East respiratory syndrome corona virus (MERS-CoV). Infection 2015; 43: 495-501.
52. Algahtani H, Subahi A, Shirah B. Neurological complications of middle east respiratory syndrome coronavirus: a report of two cases and review of the literature. Case Rep Neurol Med 2016; 2016: 3502683. doi: 10.1155/2016/3502683.
53. Hwang C. Olfactory neuropathy in severe acute respiratory syndrome: report of a case. Acta Neurologica Taiwanica 2006; 15: 26.
54. Ng KHL. Pulmonary artery thrombosis in a patient with severe acute respiratory syndrome. Postgrad Med J 2005; 81: e3.
55. Wong RSM. Haematological manifestations in patients with severe acute respiratory syndrome: retrospective analysis. BMJ 2003; 326: 1358-1362.
56. Zini G, Bellesi S, Ramundo F, et al. Morphological anomalies of circulating blood cells in COVID-19. Am J Hematol 2020; 95: 870-872.
57. Al-Tawfiq JA, Hinedi K, Abbasi S, et al. Hematologic, hepatic, and renal function changes in hospitalized patients with Middle East respiratory syndrome coronavirus. Int J Lab Hematol 2017; 39: 272-278.
58. Arabi YM, Arifi AA, Balkhy HH, et al. Clinical course and outcomes of critically ill patients with middle east respiratory syndrome coronavirus infection. Ann Intern Med 2014; 160: 389-397.
59. Tang N, Li D, WangX, et al. Abnormal coagulation parameters are associated with poor prognosis in patients with novel coronavirus pneumonia. J Thromb Haemost 2020; 18: 844-847.
60. Suh YJ, Hong H, Ohana M, et al. Pulmonary embolism and deep vein thrombosis in COVID-19: a systematic review and meta-analysis. Radiology 2021; 298: 70-80.
61. Espallargas I, Rodríguez Sevilla JJ, Rodríguez Chiaradía DA, et al. CT imaging of pulmonary embolism in patients with COVID-19 pneumonia: a retrospective analysis. Eur Radiol 2021; 31: 1915-1922.
62. Klok F, Kruip M, van der Meer N, et al. Incidence of thrombotic complications in critically ill ICU patients with COVID-19. Thromb Res 2020; 191: 145-147.
63. Chen J, Wang X, Zhang S, et al. Characteristics of acute pulmonary embolism in patients with COVID-19 associated pneumonia from the city of Wuhan. Clin Appl Thromb Hemost 2020; 26: 107602962093677.
64. Zhou J, Li C, Zhao G, et al. Human intestinal tract serves as an alternative infection route for Middle East respiratory syndrome coronavirus. Sci Adv 2017; 3: eaao4966.
65. Leung WK, To KF, Chan PK, et al. Enteric involvement of severe acute respiratory syndrome-associated coronavirus infection. Gastroenterology 2003; 125: 1011-1017.

66. Chan KH, Poon LL, Cheng V, et al. Detection of SARS coronavirus in patients with suspected SARS. Emerg Infect Dis 2004; 10: 294-299.
67. Xu H, Zhong L, Deng J, et al. High expression of ACE2 receptor of 2019-nCoV on the epithelial cells of oral mucosa. Int J Oral Sci 2020; 12: 8.
68. Vaidya T, Nanivadekar A, Patel R. Imaging spectrum of abdominal manifestations of COVID-19. World J Radiol 2021; 13: 157-170.
69. Carvalho A, Alqusairi R, Adams A, et al. SARS-CoV-2 gastrointestinal infection causing hemorrhagic colitis: implications for detection and transmission of COVID-19 disease. Am J Gastroenterol 2020; 115: 942-946.
70. Bhayana R, Som A, Li MD, et al. Abdominal imaging findings in COVID-19: preliminary observations. Radiology 2020; 297: E207-E215.
71. Goyal N, Chung M, Bernheim A, et al. Computed tomography features of coronavirus disease 2019 (COVID-19). J Thorac Imaging 2020; 35: 211-218.
72. Wong HYF, La HYS, Fong AHT, et al. Frequency and distribution of chest radiographic findings in patients positive for COVID-19. Radiology 2020; 296: E72-E78.
73. Colorado JM, Ardila LF, Vásquez NA, et al. Organizing pneumonia associated with SARS-CoV-2 infection. Radiol Case Rep 2021; 16: 2634-2639.
74. Vadász I, Husain-Syed F, Dorfmüller P, et al. Severe organizing pneumonia following COVID-19. Thorax 2021; 76: 201-204.
75. Bieksiene K, Zaveckiene J, Malakauskas K, et al. Post COVID-19 organizing pneumonia: the right time to interfere. Medicina (Kaunas) 2021; 57: 283.
76. Drakopanagiotakis F, Polychronopoulos V, Judson MA. Organizing pneumonia. Am J Med Sci 2008; 335: 34-39.
77. Waller JV, Allen IE, Lin KK, et al. The limited sensitivity of chest computed tomography relative to reverse transcription polymerase chain reaction for severe acute respiratory syndrome coronavirus-2 infection. Invest Radiol 2020; 55: 754-761.